THE MECHANISM AND RISK EVALUATION OF LARGE SCALE FLOW SLIDES OF LOESS DEPOSIT INDUCED BY EARTHQUAKES

L.M. Wang(1), Q. Wang(2) , P. Wang(3), X.W. Pu(4) , S. F. Chai(5), J. C. Chen(6)

(1) Professor, Lanzhou Institute of Seismology, China Earthquake Administration, wanglm2304@126.com
(2) Associate professor, Lanzhou Institute of Seismology, China Earthquake Administration, wangq0930@126.com
(3) Associate professor, Lanzhou Institute of Seismology, China Earthquake Administration, 19636855@126.com
(4) Associate professor, Lanzhou Institute of Seismology, China Earthquake Administration, wdpuxw@163.com
(5) Assistant professor, Lanzhou Institute of Seismology, China Earthquake Administration, chaishaofeng520@163.com
(6) Post-graduate, Lanzhou Institute of Seismology, China Earthquake Administration, 1368346487@qq.com

Abstract

The Loess Plateau of China is a continuous loess distribution area with largest area of 440,000 km^2, maximum thickness of 500m, most complex topography including tableland, ridge, round mound, valley and terrace, and most serious earthquake disasters causing 1.4 million people dead on the globe. The main reason why earthquakes caused so large death toll is large scale landslides, flow slides as well as seismic subsidence except poor seismic performance of houses. In the past, a lot of research on loess landslides and subsidence induced by earthquakes have been carried out. However, the mechanism of large scale flow slides induced by earthquakes has not been clarified and the risk of such a devastating geotechnical earthquake disaster has not been really recognized.

In this paper, the authors present their latest research achievements on the mechanism and risk of large scale flow slides of loess deposit induced by strong earthquakes. Three cases of large scale flow slides in loess deposit triggered by liquefaction are recognized to be respectively caused by three historical great earthquakes. In the western region of the Loess Plateau, a flow slides in an area of 1.5km wide and 9km long was triggered by liquefaction of loess deposit in Shibeiyuan, Ningxia Hui Autonomous Region during the Haiyuan 8.5 earthquake in 1920, which totally killed 270,000 people. The field investigation shown that it was raising of underground water in two days before the earthquake that saturated the loess layer at the depth of 16m and the loess deposit above this liquefied layer moved for hundreds of meters along a very gentle slope of 1.5-2 degree. The other two cases of flow slides of loess deposit occurred in Shanxi province, the eastern region of the Loess Plateau. One is the flow slides with the maximum sliding of 200m in an area of 5.5 km long and 2km wide triggered by loess liquefaction in Xunbao village, Hongtong County, during the Hongtong 8.0 earthquake in 1303, which killed 200,000 people. The liquefied loess layer within 12 m deep had been saturated by water seepage of an ancient irrigation water channel named Ho canal. The other occurred in Baotou village, Linfen city during the Linfen 8.0 earthquake in 1695, which killed 52,000 people. The flow slides separated Baotou village into two parts, Eastern Bao village and Western Bao village, with a seismic trench of 400m long, 150-200m wide and 60m deep. The trench was formed by moving of loess deposit towards to the west in a gentle slope of about 1 degree. The sand boil channels with a diameter of 20cm and 19m high shown liquefaction occurred in the loess layer 19m deep. The mechanism of flow slides triggered by liquefaction of loess deposit in a nearly flat tableland during three great earthquakes was clarified based on the field investigation, laboratory tests and numerical analysis. The risk of such a large scale flow slides in loess tableland was recognized and evaluated.

Keywords: soil flow; loess liquefaction; mechanism; risk evaluation; loess tableland

1. Introduction

An earthquake with magnitude of Mw7.5 occurred near Palu, the capital of Sulawesi province in eastern Indonesia, at 10:02 on September 28, 2018. The epicenter of the earthquake was 0.59 ° S 119.94 ° E at the north of Palu City, with a focal depth of 20 km. The earthquake resulted in large scale flow slides, caused serious damage to the Midwest of Sulawesi island. 2256 people died, 1309 people were missing, nearly 70000 houses were damaged, more than 220000 people were homeless, and the total economic loss exceeded 920 million dollars [1]. The large scale flow slides of stratum induced by this earthquake mostly occurs on the alluvial fan of Quaternary sandy clay with low slope angle. The landslide has a wide distribution area and most slip angles are ≤ 1.5 °. Along with a large amount of lateral displacement, part of the front edge of the landslide forms mud flow. The area of the three main sliding bodies around Palu is 0.3-1.4 km^2, and the maximum sliding distance is about 1.1 km. Among them, Balaroa landslide is located in the west of Palu City, close to the fault zone; Petobo landslide and Sidera landslide are located in the east of Palu city. It should be noticed that the steep slope located at the upper part of the irrigation system, and the soil moisture content is relatively low, is still stable in the earthquake, while in the slope area with low angle and underlying saturated soil layer, large scale flow slides has occurred and caused huge casualties and property losses in the earthquake. It shows that the leakage of the water conveyance channel of the irrigation system increases the groundwater level and the water content of the soil, which increases the dynamic vulnerability and liquefaction sensitivity of the soil mass. Under the action of strong earthquake, there are a lot of water accumulation and sand blasting in the flow slides area, which shows that the liquefaction of the saturated or nearly saturated stratum causes the loss of the shear strength of the soil mass. Thus, triggering the large scale flow slides of the ground layer [2-3]. This is not the first case of large scale flow slides, and same situations also occurred in the loess areas of China.

Loess is a kind of special soil widely distributed in North of China. The natural loess has aeolian characteristics. Its particle composition is mainly composed of silt particles. It has joints with vertical distribution and macropores visible to the naked eye. The soluble salt crystals are mostly cemented between soil particles, so it has strong water sensitivity and dynamic vulnerability. The previous research [4] results show that the shear strength and stiffness of loess decrease significantly in saturated or high water content state, which shows the characteristics of softening when encountering water. Under the action of strong earthquake and other dynamic loadings, the skeleton reconstruction of saturated loess is caused by pore collapse and particle rearrangement, which leads to residual deformation. The compression of pore volume causes pore water pressure to rise, effective stress to decrease, soil structure strength to further decline and liquefaction failure to occur under the continuous action of dynamic loadinging. The historical strong earthquakes and large earthquakes, for example, the Hongtong M8 earthquake in 1303 [5], the Linfen M7 ¾ earthquake in 1695 [6], and the Haiyuan Ms8.5 earthquake 1920 [7], had induced liquefaction of saturated loess, resulting in a large number of casualties and property losses due to low angle slope stratum sliding, mud flow and subsidence. The above earthquake damage examples show that the liquefaction of saturated loess has the characteristic of small triggering intensity, large scale sliding of loess stratum with low angle, and long-distance sliding, which results in serious disaster losses. In addition, laboratory tests, field blasting and engineering dynamic tamping have also confirmed the existence of loess liquefaction and the fact that it causes disasters from multiple perspectives [8-9]. However, due to the lack of detailed records about the earthquake damage of saturated loess in the historical earthquakes in the loess area, the physical process and mechanical mechanism of large scale flow slides in the loess stratum is not very clear, and the research on its main influencing factors and risk assessment is relatively lacking.

Based on the in-depth investigation and analysis of three typical flow slides cases triggered great earthquakes in the loess area of China and comprehensive research works which are drilling and trench exploration, numerical simulation, dynamic triaxial test, and theoretical analysis done in Shibeiyuan, the characteristics and the mechanical mechanism of large scale flow slides in loess deposit was clarified. Meanwhile, the probability risk evaluation method of flow slides is put forward. The research results can provide a theoretical basis for the risk evaluation of large scale flow slides disaster in loess strata, and is of certain significance for reducing the earthquake disaster in loess area.

2. Three Cases of Flow Slides in Loess Deposit

2.1 Flow slides induced by the Hongtong M8 earthquake in 1303

"Wu xing annals of the Yuan Dynasty history" records, "Fan Xuanyi, Xunbao, Zhaocheng County, Pingyang, slipped more than ten li.". This record described that the Xunbao village slipped more than 5km in the the Hongtong M8 earthquake in 1303. "Huozhou annals of Daoguang reign" contains, "Zhao Chengfan Xuanyi, Xunbao mountain moved more than ten li, and all the houses of the residents were destroyed.". This record also records the Xunbao village flow slides in the the Hongtong M8 earthquake in 1303. "China earthquake catalogue" published in 1971[10] clarified the epicenter is Zhaocheng, Hongdong, the intensity of epicenter is XI, the magnitude is M8, and more than 200,000 people died in this earthquake.

Based on the unmanned aerial vehicle (UAV) photos, we determined the boundary of Xunbao village flow slides (Fig.1). The length of sliding range is about 5.5km, the width is about 150m~2km, the thickness ranges from 1m to 30m, the sliding range is about 20km^2, the volume is about 60 million m^3, the sliding distance is about 100~200m, and the original slope angle is about 2°. According to the field investigation, the trailing edge of this flow slides along with the old canal of Ho. We speculate that the soil might be saturated by the long-term seepage of the canal before earthquake occurred.

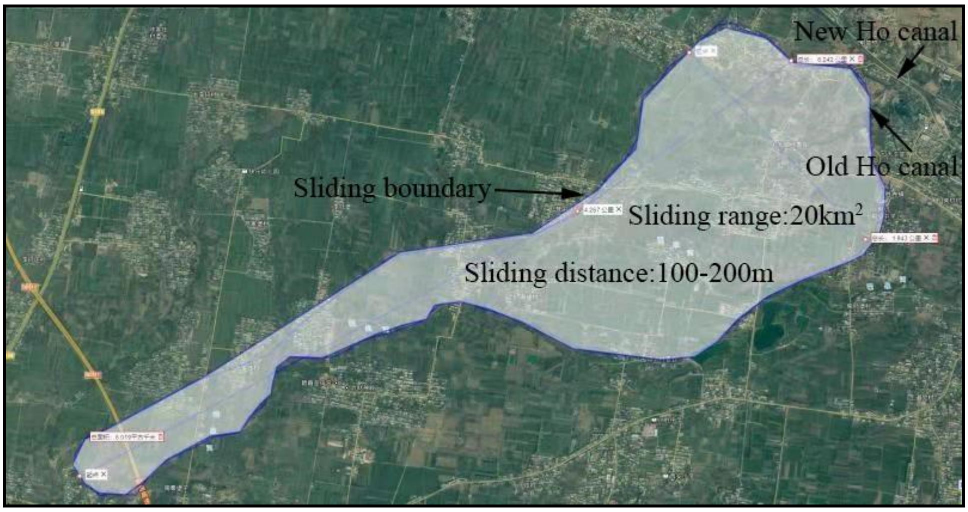

Fig. 1 – UAV photos of Xunbao village flow slides

2.2 Flow slides induced by the Linfen M7 ¾ earthquake in 1695

The epitaph of Wang Jinyin unearthed in Xibu village, Shanxi province, in the 42nd year of Qianlong reign, records "People who lived in Baotou village all year around have to move to the west of Baotou village and named it Xibu village. Because the earthquake had destroyed their houses.". It described the evolution of Baotou village under the influence of the Linfen M7 ¾ earthquake in 1695. According to the records of "China earthquake catalogue" published in 1971, the epicenter of this earthquake is Linfen, the intensity of epicenter is XI, the magnitude is M8, and more than 52,000 people died in this earthquake.

According to the field investigation and the description of local people, we infer that Dongbu village and Xibu village were originally a village and was divided by a trench (Fig.2(a)) caused by the flow slides under the Linfen M7 ¾ earthquake in 1695, which consistent with historical records. The length of trench more than 400m, the width is about 150~200m, the depth is more than 60m. The cross section of "seismic trench" [11] show the site of sand boiling (Fig.2(b)), which proved that sufficient groundwater existed below the surface when earthquake occurred.

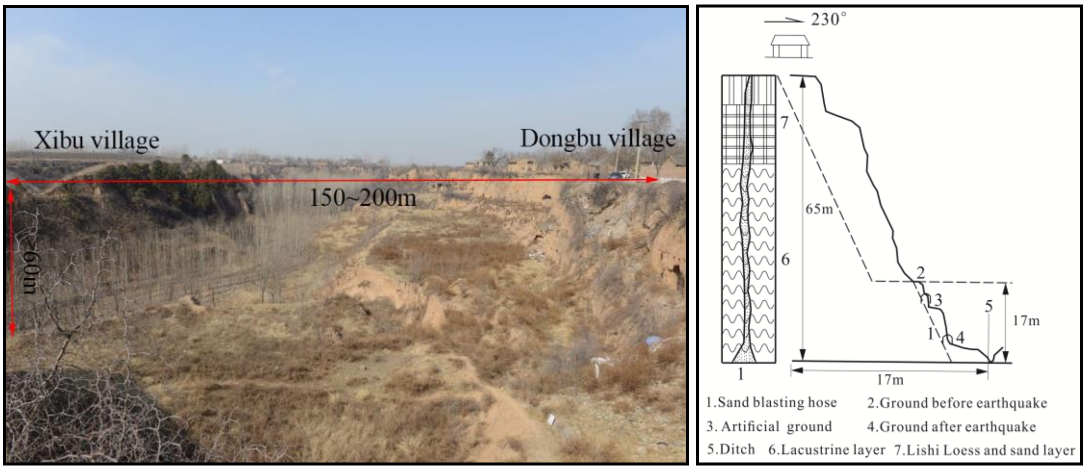

(a) (b)

Fig. 2 – The photo and Cross section of "seismic trench" between Dongbu village and Xibu village

2.3 Flow slides induced by 1920 Haiyuan Ms8.5 earthquake

On December 16, 1920, an Ms8.5 earthquake occurred in Haiyuan, Ningxia. The epicenter intensity was XII. In the low angle of Malan loess layer (Q3) of Shibeiyuan, Guyuan city, 70~90 km away from the epicenter, a large scale and long-distance flow slides occurred, resulting in extremely serious earthquake damage phenomenon [12, 13] (Figure 3). 44 households were buried and more than 200 people died in this region.

The large scale flow slides of loess stratum induced by the earthquake occurred on the low and gentle slope composed of the second and third terrace. The length of slide area is about 2.1km from south to north, the width is about 1.2~1.3km from east to west, and the influenced range is about 2km^2. The underground water in this area is sufficient. The mechanism of large scale flow slides in this area will be discussed later.

Fig. 3 – The flow slides damage phenomenon of loess deposit in Shibeiyuan region

3. The Mechanism of Flow slides in Loess Deposit

3.1 Drilling and trench exploration in the site of Shibeiyuan large scale flow slides

In order to study the mechanism of large scale flow slides in loess deposit, a series of in site works has been down in Shibeiyuan, Haiyuan. According to the remote sensing image and field photo of Shibeiyuan large scale flow slides, the basic situation about this area be described as following. The main sliding direction is 330°, the thickness of sliding body is about 10-30m, the volume is about 40 million m^3. The trailing edge of flow slides show the characteristic of higher in the north and lower in the south. Eight drilling and one trench were carried out in this area and shown in Fig. 4(a). The field photos of drilling and trench are shown in Fig. 4(b) and Fig. 4(c).

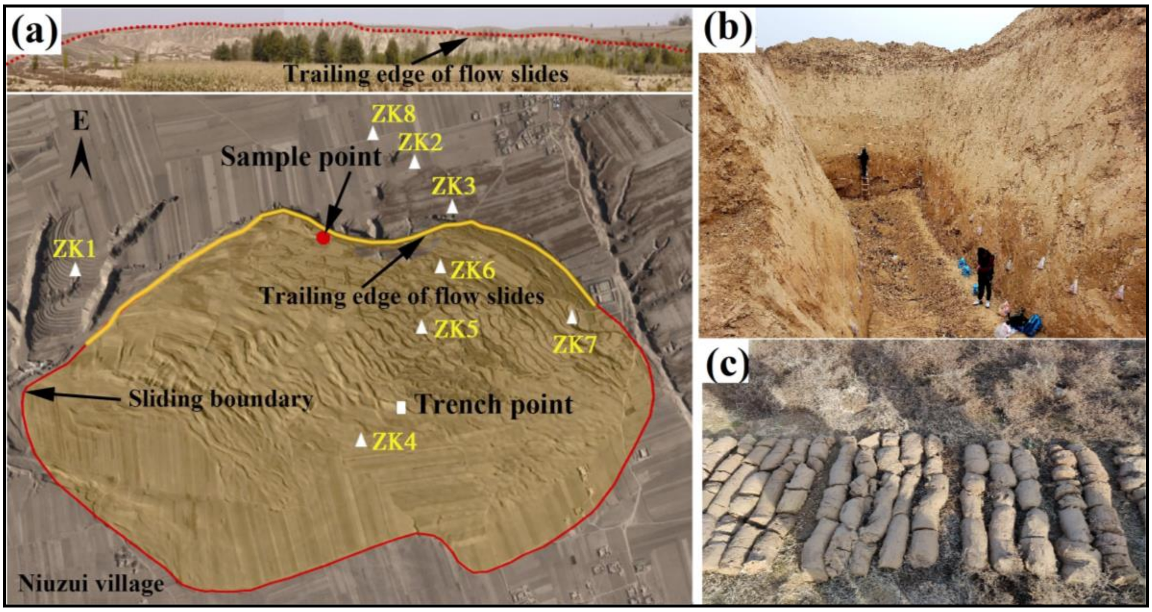

Fig. 4 –(a)The layout of drilling and trench in Shibeiyuan; (b), (c)Field photos of drilling and trench

According to the data of drilling ZK3, ZK4, ZK5, and ZK6 which along the sliding direction, the cross section and stratum structure of Shibeiyuan flow slides were figured and shown in Fig 5. Fig 5 shows that from the top to the bottom, the landslide area of shibeiyuan is divided into Q3 late Pleistocene Malan loess layer and Middle Pleistocene Q2 Lishi loess layer. The second paleosol layer is the boundary between the two layers, and different types of loess layers are gradually thinning from the trailing edge to the front edge. Q3 Malan loess layer can be divided into the following four layers from top to bottom. The first layer is the upper unsaturated loess layer. The thickness of it in the plateau top area is about 14 m, and the front edge is about 1-2 m, the loess structure of this layer is loose, the large pores of the support are developed, the engineering mechanical properties are weak, and it has strong dynamic vulnerable characteristics. Because it is covered on the surface, the water content is low, and under the dynamic action, it is easy to produce brittle failure forms such as tension crack and shear off. The second layer is the first paleosol layer. This layer with depth about 15 m and the thickness is about 1 m at the trailing edge and it has a large clay content and poor water permeability. The third layer is the sandy loess layer. This layer with depth about 16 m and the thickness is about 15 m at the trailing edge. The fourth layer is the fine sand layer with the thickness of 0.2m and located in the middle of sandy loess layer. Middle Pleistocene Q2 Lishi loess layer can be divided into the following two layers from top to bottom. The first layer is the second paleosol layer. This layer with depth about 27 m and the thickness is about 1 m at the trailing edge. The second layer is the loess layer. Above results show that the sandy loess layer in the stratum has a high liquefaction potential, and there are two layers of Paleosol layers above and below it. Because of the poor permeability of paleosol, when the sandy loess layer is liquefied, the instantaneous rise of pore water pressure will be blocked by the paleosol layer and converged in the paleosol layer and its lower part, forming a soft weak slip surface, and the upper soil is prone to slide under the action of seismic force.

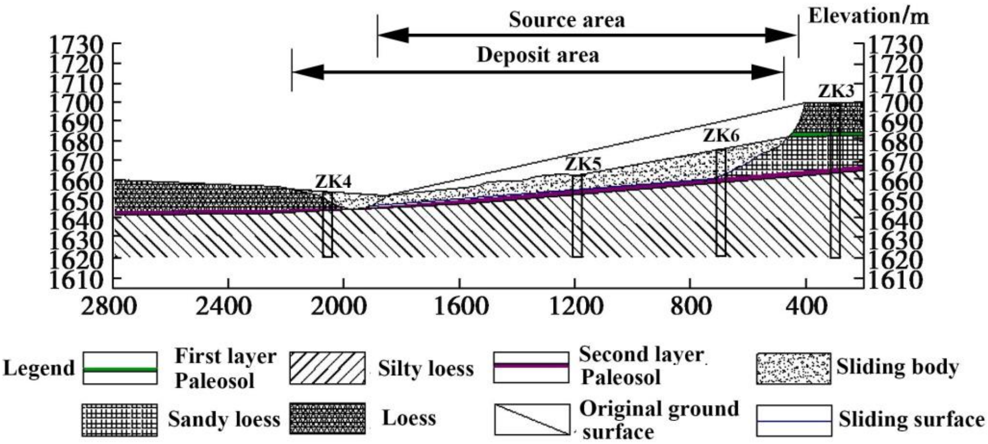

Fig. 5 – Cross section and stratum structure of Shibeiyuan flow slides

In order to study the sliding mechanism of flow slides in Shibeiyuan, a 12 m deep and 21 m long trench was also been excavated. The location of the trench in the sliding area is shown in Fig 4 (a). The peak width is about 10-15 m and the valley width in this location is about 8 m. According to the final form of trench, the simple profile of trench was figured and shown in Fig 6. Fig 6 shows that the peak stratum is composed of the upper unsaturated loess, the first paleosol layer, and the lower sandy loess liquefaction layer, while the valley is mainly composed of the lower sandy loess liquefaction layer and the upper arable soil. There is a discontinuous sand layer in the lower part of peak and valley. The flow pattern of the liquefiable layer is obvious. The water content of the liquefiable layer is about 20%-22%, while that of the first paleosol is 14%-19% from top to bottom. The paleosol layer is generally in parallel and integrated contact with the upper and lower strata, but there are many wave peaks and wave valleys in the paleosol layer of the trench, which show that it suffered the effect of top squeezing of the lower liquefied sandy loess in the process of sliding. The upper unsaturated loess layer is squeezed by the lower soil layer, and its deformation characteristics are obvious, but it still maintains the basic sedimentary sequence.

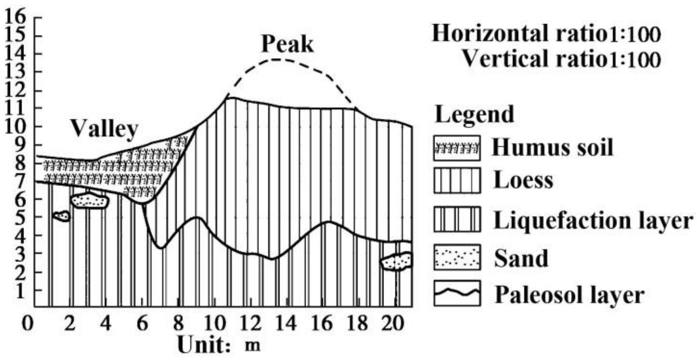

Fig. 6 – Simple profile of trench in Shibeiyuan flow slides

3.2 Numerical analysis based on Finite element method

According to the stratum structure of Shibeiyuan before sliding, the finite element numerical analysis model is established. The stratum including the upper unsaturated loess, the middle saturated sandy loess and the lower Q2 Lishi loess. The Wenchuan earthquake wave recorded by Tangyu station is loaded. The boundary of infinite element is on both sides of the model. The physical and mechanical parameters of soil in different layers are assigned according to the measured data. See Table 1 for the specific parameters

Table 1 – Physical and mechanical parameters of soils

Layers	Density /(g·cm^3)	Elastic modulus /MPa	Poisson ratio	Cohesive force/kPa	Internal friction angle/(°)
Upper unsaturated loess	1.35	55	0.27	23	26
Saturated sandy loess	1.65	80	0.26	12	16
Q2 Lishi loess	1.72	120	0.23	62	25

The results show that there is no residual deformation in different parts of the slope under the effect of 100 gal (VII). Under 200 gal (VIII), the saturated sandy loess layer has significant residual deformation, with local deformation more than 3% (Fig. 7 (a)), indicating that the soil is partially liquefied, and the unsaturated loess at the slope shoulder has lost part of its supporting force due to the downward residual deformation of the lower saturated sandy loess, but the stress variable is within 2%, so no crack failure has occurred. The unsaturated loess in the upper part of the slope moves along the slope due to liquefaction of the middle sandy loess layer and the downward subsidence, and flow drag, but the total accumulated displacement is 0.56 m (Fig. 7 (b)), so there is no large scale sliding of the soil under this condition. At 600 gal (IX), 10%-14% of the residual deformation occurs in the sandy loess layer at the middle and upper parts of the slope (Fig. 7 (c)), the residual deformation at the middle and lower parts also exceeds 3%, and the total accumulated displacement is 3.43 m (Fig. 7 (d)), indicating that the whole saturated sandy loess layer is liquefied due to seismic ground motion. Due to the large liquefaction deformation of the soil in the upper part of the slope, the liquefaction layer in this part will sink and flow along the slope, which makes the unsaturated loess in the slope shoulder appear brittle tension shear fracture due to the reduction of the lower supporting force, the traction of the soil in front and the earthquake inertia force. Due to the tension shear fracture of slope shoulder, the soil mass in the upper part of the slope loses the connection function of the parent body of the trailing edge. The seismic inertia force and gravity sliding force drive the soil sliding greatly.

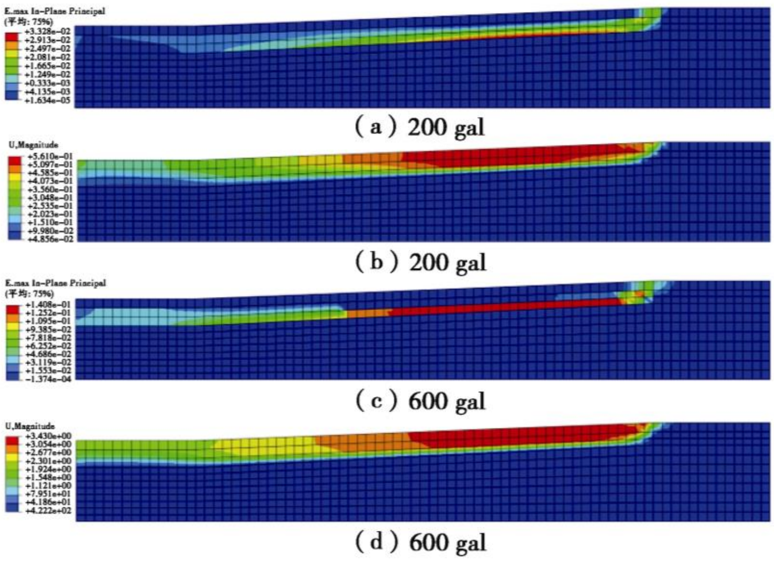

Fig. 7 – Contour of strain and displacement under different intensities (Unit: m)

3.3 Liquefaction mechanism of saturated loess

In order to study the liquefaction characteristics of saturated loess, the dynamic deformation and pore water pressure evolution of saturated loess under cyclic loading are studied by dynamic triaxial tests.

The soil samples used in the test are taken from different sites of the Loess Plateau, all of which are Q3 loess, with a sampling depth of 4-5m. The main physical property parameters of the samples are shown in Table 2. As a typical structural special soil, the liquefaction of saturated loess is mainly determined by its physical and mechanical properties, microstructure characteristics, water and electrochemical properties, and the combined action of cyclic loading and water is the main factor leading to the liquefaction failure of saturated loess. Fig. 8 shows the cyclic shear effective stress paths of saturated loess in different regions. It can be seen from Fig. 8 that the effective stress path of saturated loess in cyclic shear process is approximately inclined linear change, and the average effective stress gradually decreases with the increase of dynamic pore water pressure, but the effective stress of saturated loess in different areas does not decrease to 0 point when it is damaged, namely, it does not reach the initial liquefaction state. The average effective stress of soil decreases monotonously before the partial stress decreases, and the shape of stress path has no obvious change; after the partial stress decreases obviously, the average effective stress continues to decrease monotonously, and after the liquefaction failure of soil, it presents a decrease to increase cyclic change law. The average effective stress of MH loess decreases slowly under cyclic loading, and decreases rapidly at the initial stage of cyclic loading, then tends to be stable; with the continuous decrease of mean effective stress, the deceleration rate of partial stress increases gradually, and increases rapidly when the mean effective stress reaches about 70 kPa. Under the cyclic shear action, the average effective stress of LX loess increases monotonically and accelerates before the liquefaction failure of the sample, and the partial stress attenuation is nearly linear, but the attenuation rate is relatively small; after the liquefaction failure, the decrease increase of the average effective stress changes obviously in the cyclic, and the minimum value of the average effective stress is about 35 kPa. In the initial stage of cyclic shear, the average effective stress of ty loess decreases slowly, and the rate of decrease increases with the acceleration of the accumulation rate of dynamic pore water pressure; the partial stress decreases linearly with the decrease of average effective stress, and decreases rapidly when the average effective stress reaches 80 kPa, and decreases slowly and tends to be stable when the average effective stress reaches 60 kPa; cyclic shear At the end of the shear period, the average effective stress and the rate of deviator stress decline are relatively slow, and the stress path shape gradually tends to be stable. The minimum value of average effective stress is 10 kPa, and the minimum value of deviator stress is about 5 kPa.

Table 2 – Physical and mechanical parameters of loess samples

Sample number	**Location**	**Density /(g·cm^{-3})**	**Dry density /(g·cm^{-3})**	**Water content /%**	**Plasticity index**	**Particle composition /%**		
						Clay	**Silt**	**Sand**
LX	Linxia, Gansu	1.33	1.25	5.43	9.9	18.5	74.0	7.5
TY	Taiyuan, Shanxi	1.37	1.30	5.46	13.5	28.5	65.6	5.9
MH	Minhe, Qinghai	1.59	1.42	12.25	9.8	22.0	57.8	20.2

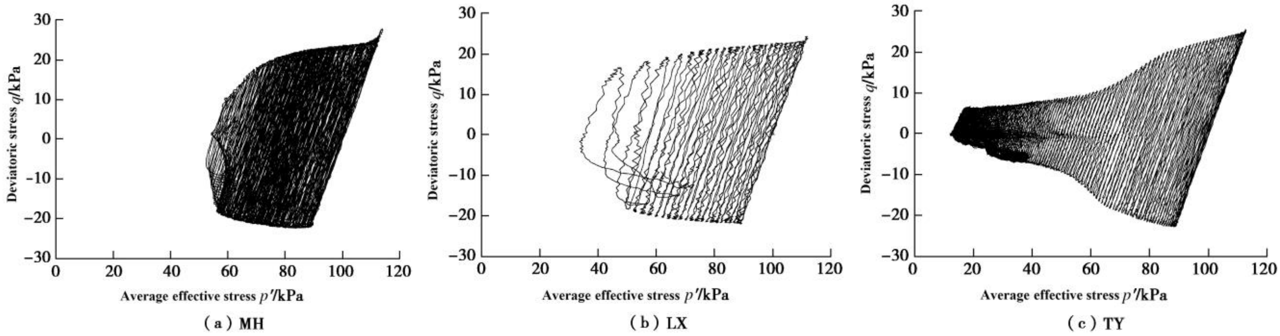

Fig. 8 – Effective stress paths of saturated loess in different areas

The dynamic triaxial test results shown in Fig. 9 show that with the increase of water content, the dynamic cohesion and dynamic internal friction angle of Lanzhou loess decrease nonlinearly. In the saturated state, the dynamic cohesion and dynamic internal friction angle decrease to 50% and 70% of the original loess respectively. However, for the saturated soil, most of its structural strength remains, and the soil skeleton is in a sub stable state.

Therefore, the internal mechanism of liquefaction failure of saturated loess under dynamic loading is mainly the response of soil skeleton to cyclic loading and the adaptive response of water in soil to pore deformation due to the response of soil skeleton, which leads to the alternating action of weakening of soil skeleton strength and increasing of pore water pressure, until the soil loses its structural strength and behaves as an approximate fluid state.

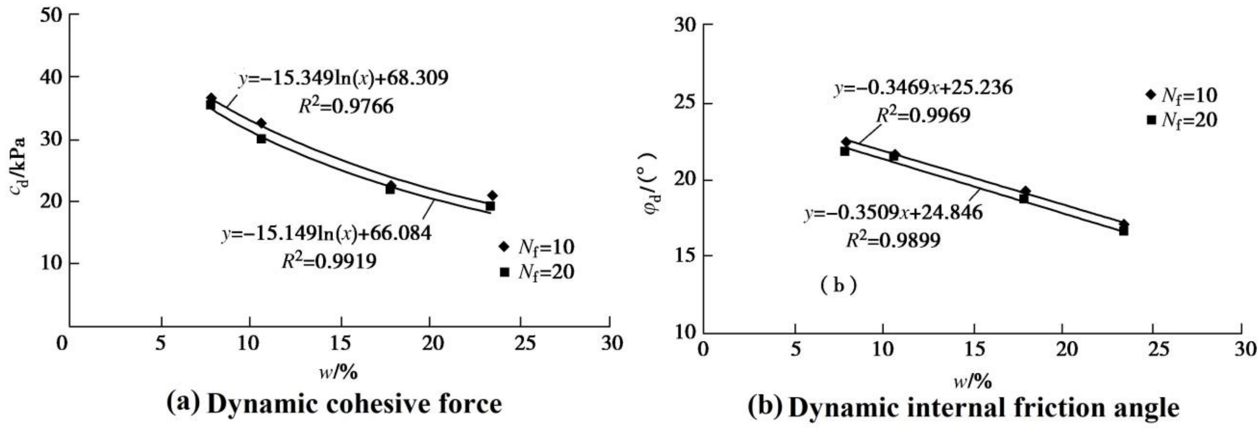

Fig. 9 – Dynamic cohesion force and dynamic internal friction angle change rules of Lanzhou loess under different water contents

3.4 The Mechanism of large scale flow slides in loess deposit

Based on the field investigation, large scale trench and drilling exploration, dynamic triaxial test, theoretical analysis, and numerical simulation calculation, the mechanism of large scale flow slides of loess stratum in Shibeiyuan caused by Haiyuan Ms8.5 earthquake in 1920 is revealed as follows (Fig. 10).

A few days before the Haiyuan earthquake, according to the many local villagers' reports and literature records [14], the water level of the well rose to about 15 m, that is, the loess stratum below 15 m depth was in a state of water saturation. During the earthquake, the sliding zone is located in the X area. Under the action of earthquake, the sandy loess layer under the first paleosol layer liquefied, the pore water pressure rose, and the liquefiable materials flowed up. When the pore water flowed up to the first paleosol layer, due to the poor permeability of the layer, it was blocked and gathered under the first paleosol layer, and a thin layer of water film was formed instantly. The water film, high moisture content paleosol layer, and liquefied sandy loess layer, might form a large area of sliding surface (belt). Under the coupling effect of seismic inertia force and sliding force of 2 ° gentle slope, the overlying soil slid to northwest along the inclined direction of the gentle slope in the Loess Plateau. Due to the combined action of the movement of the sliding soil and the upwelling of liquefied materials, the waved topography was formed, where the sliding soil forms a valley at the cracking position and a peak at the deposit area.

This mechanism has also been verified by the field investigation of the large scale flow slides of loess stratum caused by the Hongdong M8 earthquake in 1303 and the Linfen M8 earthquake in1695.

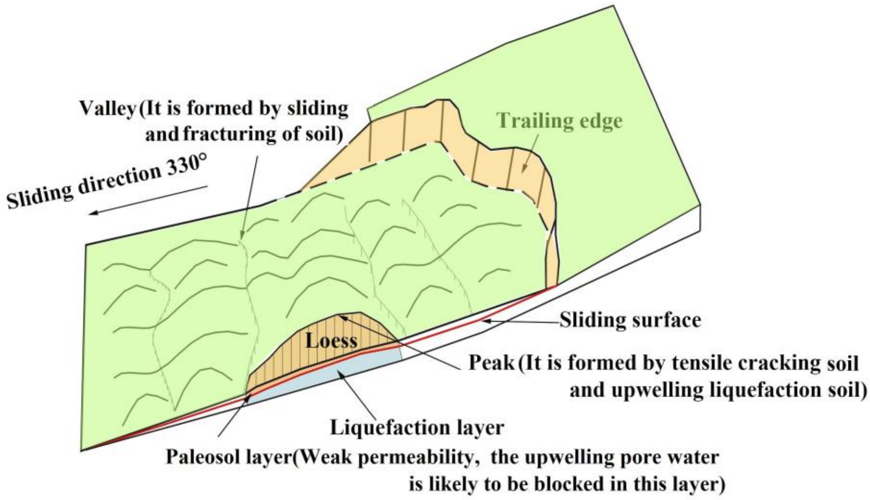

Fig. 10 – Diagrammatic sketch of mechanism of flow slides of loess deposit in Shibeiyuan

4. Risk Evaluation of Flow Slides in Loess Deposit

The distribution of Loess Plateau in China shown in Fig.11(a). The Loess Plateau is located in the north of China, with a total area of 517489 km^2 including its vicinity. The width of it is about 750 km from north to south and the length is about 1000 km from east to west. The average thickness of loess in the area is 50-80 m, and the maximum thickness is 150-500 m. Probability risk evaluation method is a safety assessment method, such as the minimum disaster acceleration method, which is based on the triggering probability of a certain basic causing factor and through the mathematical statistics probability analysis method, to obtain the correlation degree (or importance degree) of the basic causing factor of the disaster or the accident probability of the whole assessment system.

Considering the fifth generation of Seismic Ground Motion Parameter Zoning Map of China (2015) [15] and the range of different seismic peak acceleration values in combination with the Loess distribution, the flow slides risk map under the corresponding probability is compiled shown in Fig.12. Under the condition of 10% exceedance probability in 50 years (Fig.11(b)), the total area of I risk area is about 160877 km^2, accounting for 31.09% of the area of the Loess Plateau, which is concentrated in the east of Gansu Province, Ningxia Hui Autonomous Region, the middle of Shaanxi Province, Shanxi Province and Hulunbuir city of Inner Mongolia Autonomous Region. The total area of II risk area is about 14546 km^2, accounting for 2.81% of the area of the Loess Plateau, which are concentrated in Tianshui City, Guyuan City Linfen City, and Zhongwei city. The total area of level III risk area is about 437 km^2, accounting for 0.08% of the area of the Loess Plateau, which is concentrated in the Haiyuan earthquake fault zone of Guyuan City. Under the condition of 2% exceedance probability in 50 years (Fig.11(c)), the total area of I risk area is about 189575 km^2, accounting for 36.63% of the area of the Loess Plateau, which is concentrated in the east of Gansu Province, Ningxia Hui Autonomous Region, the middle of Shaanxi Province, Shanxi Province and Hulunbuir city of Inner Mongolia Autonomous Region. The total area of II risk area is about 31676 km^2, accounting for 6.12% of the area of the Loess Plateau, which are concentrated in Tianshui City, Guyuan City Linfen City, and Zhongwei city. The total area of III risk area is about 1048 km^2, accounting for 0.20% of the area of the Loess Plateau, which is concentrated in the Haiyuan earthquake fault zone of Guyuan City. Under the condition of 0.5% exceedance probability in 50 years (Fig.11(d)), the total area of I risk area is about 284668 km^2, accounting for 55.01% of the area of the Loess Plateau, which is concentrated in the east of Gansu Province, Ningxia Hui Autonomous Region, the middle of Shaanxi Province, Shanxi Province and Hulunbuir city of Inner Mongolia Autonomous Region. The total area of II risk area is about 64008 km^2, accounting for 12.37% of the area of the Loess Plateau, which are concentrated in Tianshui City, Guyuan

City, Linfen City, and Zhongwei city. The total area of III risk area is about 2219 km^2, accounting for 0.43% of the area of the Loess Plateau, which is concentrated in the Haiyuan earthquake fault zone of Guyuan City.

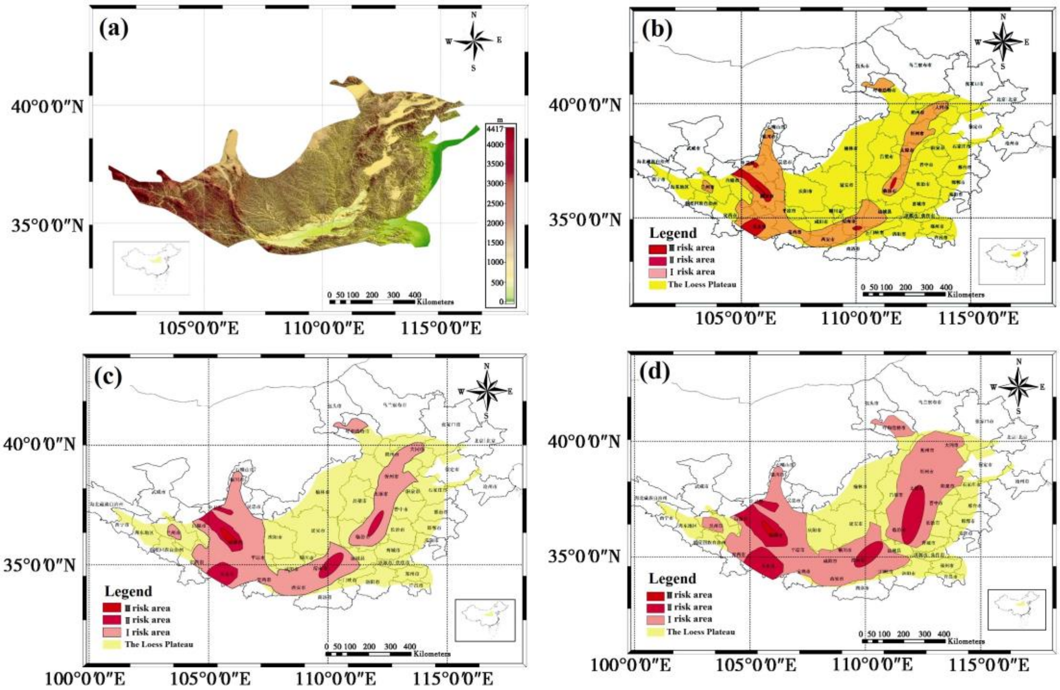

Fig. 11 – Risk zoning map of flow slides in Loess Plateau ((a) The distribution of Loess Plateau. (b)exceedance probability: 10% in 50 years; (c) 2% in 50 years; (d) 0.5% in 50 years.)

5. Conclusions

Based on field investigation and analysis of three typical flow slides cases and comprehensive further research works done in Shibeiyuan, the characteristics and the mechanism of large scale flow slides in loess deposit was clarified. The probabilistic risk evaluation of flow slides is carried out. The main conclusions are as follows:

(1) The three liquefaction-triggered flow slides in loess area show the characteristics of large scale, long sliding distance, and heavy casualties. Before earthquake, the loess deposit within a certain depth is saturated or nearly saturated because of the ground water rises or the long-term water seepage of canal.

(2) The internal mechanism of liquefaction failure of saturated loess is mainly the response of soil skeleton to the dynamic loading and the adaptive response of water in the soil to the pore deformation, which leads to the weakening of soil skeleton strength and the increase of pore water pressure, until the soil loses the structural strength and shows the pattern of approximate flow.

(3) The mechanism of large scale flow slides of Shibeiyuan is as follows: Firstly, under the action of high-intensity ground motion, the saturated sandy loess stratum liquefies; Secondly, under the coupling effect of continuous earthquake inertia force and gravity, the liquefied soil stratum carries and drags the upper unsaturated loess stratum to produce large scale flow slides. In the process of downward movement of the surface unsaturated loess layer, there is a obvious velocity non synchronization phenomenon between different parts of the soil mass due to the reciprocating action of ground motion and the upwelling of liquefied materials, resulting in the local tensile stress concentration and the occurrence of sliding and fracturing damage, thus forming a waved topography with peaks and valleys.

The risk zoning maps of large scale flow slides in Loess Plateau of China under different exceedance probabilities are complied. The results show that the area near active fault zones has higher risk of flow slides under the three kinds of exceedance probabilities, 10%, 2%, and 0.5% in 50 years.

6. Acknowledgements

This paper is funded by National Natural Science Foundation of China (Grant No. U1939209 and 51478444).

7. References

[1] SASSA S, TAKAGAWA T (2019). Liquefied gravity flow-induced tsunami: first evidence and comparison from the 2018 Indonesia Sulawesi earthquake and tsunami disasters[J]. *Landslides*, 16(1): 195–200.

[2] BRADLEY K, MALLICK R, ANDIKAGUMI, et al (2019). Earthquake- triggered 2018 Palu Valley landslides enabled by wet rice cultivation[J]. *Nature Geoscience*, (12): 935–939.

[3] WATKINSON I M, HALL R (2019). Impact of communal irrigation on the 2018 Palu earthquake-triggered landslides[J]. *Nature Geoscience*, (12): 940-945.

[4] WANG Lan-min. Loess Dynamics[M] (2003). Beijing: Seismological Press. (in Chinese)

[5] ZHAO Jin-quan, ZHANG Da-wei, GAO Shu-yi, et al (1995). Huanbu ground slide, the relic of 1303 Hongtong, Shanxi, earthquake of *M*8[J]. *Earthquake Research in Shanxi*, (3): 17–23. (in Chinese)

[6] SU Zong-zheng, SHI Zhen-liang (1995). Study and discussion for the historical documents of Linfen Macroquake in 1695[J]. *Earthquake Research in Shanxi*, (3/4): 150–158, 169. (in Chinese)

[7] BAI Ming-xue, ZHANG Su-min (1990). Loess liquefaction flow in high intensity earthquake[J]. *Geotechnical Investigation and Surveying*, 20(6): 1–5. (in Chinese)

[8] WANG Lan-min, LIU Hong-mei, LI Lan (2000). Laboratory study on the mechanism and behaviors of saturated loess liquefaction[J]. *Chinese Journal of Geotechnical Engineering*, 22(1): 89–94. (in Chinese)

[9] WANG L M, HE K M, SHI Y C, et al (2002). Study on liquefaction of saturated loess by in-situ explosion test[J]. *Earthquake Engineering and Engineering Vibration*, 1(1): 50–56.

[10] Office of the Central Seismological working group (1971). *China earthquake catalogue* [M]. Beijing: Science Press.

[11] CHEN G S, WANG G Q (1985). Vestige of the strong Linfen earthquake of 1695, Shanxi province, and discussion of some associated problems. *Journal of seismological research*,8(5).

[12] BAI Ming-xue, ZHANG Su-min (1990). Loess liquefaction flow in high intensity earthquake[J]. *Geotechnical Investigation and Surveying*, 20(6): 1–5. (in Chinese)

[13] WANG Qian, WANG Jun, WANG Lan-min, et al (2014). Discussion on mechanism of seismic liquefaction of sturation loess in Shibei Tableland, Guyuan City[J]. *Chinese Journal of Rock Mechanics and Engineering*, 33(S2): 4168–4173. (in Chinese)

[14] State Seismological Bureau, Lanzhou Institute of Seismology (1980), Seismological Team of Ningxia Hui Autonomous Region. The Haiyuan Great Earthquake in 1920[M]. *Beijing: Seismological Press*. (in Chinese).

[15] Seismic Ground Motion Parameter Zoning Map of China: GB 18306—2015[S]. *Beijing: China Standard Press*, 2015. (in Chinese)

